Activation of β_2-Adrenergic Receptor Induced by Three Catecholamine Agonists: a Docking and Molecular Dynamics Study

ZHANG Rui[1,2], DONG Li-hua[2], LING Bao-ping[3], WANG Zhi-guo[2] and LIU Yong-jun[2,3*]

1. Shandong Key Laboratory of Edible Mushroom Technology, School of Life Sciences, Ludong University, Yantai 264025, P. R. China;

2. Key Laboratory of Adaptation and Evolution of Plateau Biota, Northwest Institute of Plateau Biology, Chinese Academy of Sciences, Xining 810008, P. R. China;

3. School of Chemistry and Chemical Engineering, Shandong University, Jinan 250100, P. R. China

Abstract We studied the activation of β_2-adrenergic receptor(β_2AR) by norepinephrine, epinephrine and isoproterenol using docking and molecular dynamics(MD) simulation. The simulation was done on the assumption that β_2AR was surrounded with explicit water and infinite lipid bilayer membrane at body temperature. So the result should be close to that under the physiological conditions. We calculated the structure of binding sites in β_2AR for the three activators. We also simulated the change of the conformation of β_2AR in the transmembrane regions(TMs), in the molecular switches, and in the conserved DRY(Aspartic acid, Arginine and Tyrosine) motif. This study provides detailed information concerning the structure of β_2AR during activation process.

Keywords β_2-Adrenergic receptor(β_2AR); G Protein coupled receptor(GPCR); Molecular dynamics; Agonist; Activation

Article ID 1005-9040(2012)-03-493-07

1 Introduction

β_2-Adrenergic receptor(β_2AR) is one of the most thoroughly investigated G protein coupled receptors(GPCRs)[1,2], which plays crucial roles in the regulation of cardiovascular functions. β_2AR can be activated by catecholamines, such as epinephrine(EPI), norepinephrine(NE), and isoproterenol (ISO)[3]. Fluorescence studies with purified human β_2AR revealed that different agonists could stabilize β_2AR with different conformations[4]. As for EPI, NE, and ISO, they may stabilize kinetically distinct active conformational states[5].

For years, experimental researchers have focused their studies on the effect of ligands on β_2AR activation[4—11], of which Kobilka and his co-workers[4—10] made great contributions in this aspect. The studies of GPCRs in depth require their exact three-dimensional structures, but they are very difficult to obtain despite of many efforts[12]. Before the successful crystallization of the human β_2AR, the application of structure-based drug discovery to GPCRs has largely been limited to the use of rhodopsin-based homology models[13]. The crystal structure of human β_2AR was firstly obtained in 2007[14,15], namely, after seven years of the settlement of the first crystal structure of GPCRs-rhodopsin[16]. As an important milestone, the discovery of human β_2AR structure made it possible to investigate the specific function of β_2AR at atomic level[17]. During the recent years, many researchers have used computational methods to study the ligands binding and β_2AR activation[18—22]. In these theoretical studies, people set up a membrane bilayer environment and performed molecular dynamics(MD) simulation to explore the different conformational changes of β_2AR. However, the multistep activation processes are still unclear[23,24].

We chose three β_2AR full agonists: two endogenous catecholamines——NE and EPI, and a prototypical synthetic agonist——ISO, to study the changes of the conformation of β_2AR in the activation processes and activation mechanism (Fig.1). The MD simulation was used to explore the active characteristics.

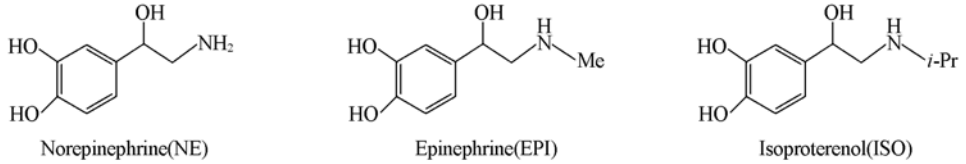

Fig.1 Structures of three agonists

*Corresponding author. E-mail: yongjunliu_1@sdu.edu.cn

Received September 19, 2011; accepted February 4, 2012.

Supported by the Young and Middle-Aged Scientists Research Awards Foundation of Shangdong Province, China(No. BS2011SW002) and the Research Foundation for Advanced Talents of Ludong University, China(No.LY2011017).

2 Computational Details

2.1 Preparation of Ligands, Receptor and Docking

2.1.1 Preparation of Ligands

The structures of NE, EPI and ISO were fully optimized at the level of 6-31G(*d*) by employing the Becke-3-parameter-Lee-Yang-Parr(B3LYP) hybrid density functional theory with Gaussian 03 package[25]. Considering the actual physiological conditions, we used the protonated structures of these ligands.

2.1.2 Preparation of Receptor

The crystal structure of the complex human β_2AR containing an inverse agonist(Carazolol) and T4-lysozyme was downloaded from Protein DataBase(PDB ID code: 2RH1)[15]. T4-lysozyme and crystallographic water molecules which were not hydrogen-bonded with β_2AR were deleted in the treatment of receptor, and then the incomplete residues in β_2AR were repaired. No reconstruct was done for the third intracellular loop(ICL3) of β_2AR(the highly flexible 43 residues between TM5 and TM6), due to the lack of appropriate template to perform homology modeling[26—28]. In addition, the removal of ICL3 in experiment did not appear to affect the function of β_2AR[29].

All the histidine residues and R131 in β_2AR were protonated, other residues were in their default ionization states[15,22,30]. These changes of ionization states were carried out by the Gromacs software. Then, the prepared structure was energy minimized before docking.

2.1.3 Parameter Setting for Docking

Docking was performed *via* the program AutoDock 4.0[31,32] with a rapid energy evaluation, in which the affinity potentials of grids were precalculated with a variety of search algorithms to find the suitable binding positions. We kept β_2AR as rigid and set all the torsional bonds of the ligands to rotate freely. A grid of 72×72×72 points was generated with a grid spacing of 0.0375 nm around the binding site, indicating a volume space of 19.68 nm^3. We performed fifty runs of independent docking for each ligand. The binding mode with the highest binding energy in the largest cluster was chosen for the following MD simulation.

2.2 Dynamics Simulations

2.2.1 Building Model

The structures of complexes of NE-β_2AR, EPI-β_2AR and ISO-β_2AR, which were obtained from docking, were embedded in the center of a square periodic lipid bilayer consisting of 280 dioleoyl phosphatidyl choline(DOPC) molecules. We deleted the overlapped DOPC molecules and at last kept 188 lipid molecules in the lipid bilayer. The resulting systems were solvated with *ca*. 21000 simple point charge(SPC) water molecules and then neutralized by counter ions at random positions. This generated a system of *ca*. 73600 atoms.

2.2.2 Gromacs Dynamics Setup

Molecular dynamics simulation was carried out by means of Gromacs V4.0.4 with the Gromos 96 force field[33]. PRODRG 2.5 Server[34] was used to parameterize the ligands. Each complex was energy minimized for 1000 steps of steepest descents, followed by a 200 ps NVT(constant number of particles, volume and temperature) equilibration phase and 500 ps position restraining NPT(constant number of particles, pressure and temperature) phase to equilibrate the system. After the initial equilibration, the restraints were removed, then, each system was subjected to a 20 ns production run. We performed 15 ns MD simulation at 300 K for NE-β_2AR system. We followed the trajectory and carried out another 20 ns MD simulation at 310 K(the body temperature of human being). After 3 ns, the root mean square distance(RMSD) of NE-β_2AR system was inclined to stabilization, and thus we only performed 20 ns simulation. The other two systems also achieved their stable conformation after 20 ns MD simulation. In order to confirm the accuracy of MD simulation, each system was computed three times.

The Berendsen coupling was used to maintain a constant temperature of 310 K and a constant isotopic pressure of 10^5 Pa. Van der Waals interaction was modeled *via* Lennard-Jones 6-12 potentials with a 1.3 nm cut-off. Long-range electrostatic interaction was calculated by virtue of the Particle Mesh Ewald method with a cut-off of 1.2 nm. And the time step was 2 fs. Analysis of the simulations was performed with Gromacs packages. Molecular graphics images were generated by Chimera program[35].

3 Results and Discussion

3.1 Docking

Literature of cell-based and biophysical studies[1,2] show that the structurally diverse agonists induce distinct conformational states of GPCRs. We studied the binding sites of the three agonists by docking(Fig.2). It can be seen that the three agonists are almost overlapped because of the structural similarity. The surrounding residues of the binding site of agonists are D113, V114, N312, S207, Y316, F289 and T118. Because the amine groups on agonists are protonated, all the agonists locate in an electrostatically negative region. We have found

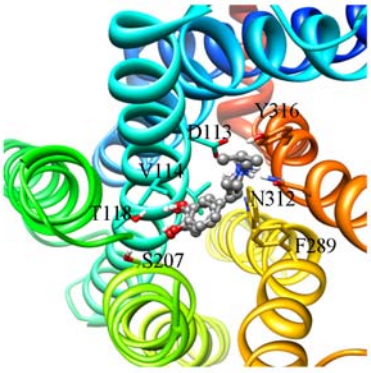

Fig.2 Top view of docking positions of NE, EPI and ISO in β_2AR

All the agonists in Fig.2 are colored by elements and shown in balls and sticks. β_2AR is shown in colored ribbons. The surrounding residues in the binding site are shown in sticks and C atoms are colored by ribbon colors, other atoms are colored by element.

that the main residues(except N293) are similar to those obtained by Swaminath *et al*.[10]. But we can't reconcile the calculated binding sites of agonists with their result[10]. The initial structure of docking was in its inactive state; while the agonists closely bond to the active structure. We also calculated the binding energies of NE, EPI, and ISO to be –35.82, –35.40, and –30.50 kJ/mol, respectively. In the following experiments we shall calculate the detailed binding site and binding mode of agonists by MD simulation.

3.2 Molecular Dynamics Simulations

3.2.1 Structural Stability of Agonist-β_2AR Systems

The root mean square distances(RMSDs) of agonist-β_2AR systems: RMSDs of EPI and ISO relative to β_2AR are *ca*. 0.35—0.4 nm, and the RMSD of NE relative to β_2AR is close to 0.6 nm. The RMSD values of β_2AR relative to itself are 0.25—0.3 nm for the RMSDs of EPI and ISO while 0.41 nm for NE(Fig.3). We attribute the differences to the frameworks of agonists: NE is the smallest molecule among the three agonists, corresponding to the largest mobility in the binding pocket.

3.2.2 Binding Sites of Agonists

Interaction of agonists with surrounding residues within 0.5 nm: starting from the docking conformations, we performed 20 ns MD simulation and obtained the stable binding sites of the three agonists. For each system, the simulation was repeated three times and very similar trajectories were obtained. Therefore, we used one typical trajectory for analyzing. The conformations of MD simulation were averaged from the final 2 ns and energy-minimized *via* the Gromacs software.

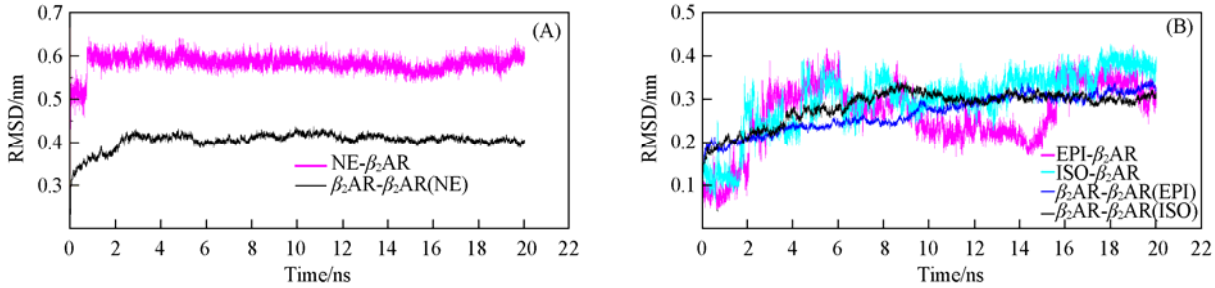

Fig.3 Drift of protein and ligands from the initial model and fluctuations of protein coordinate for NE-β_2AR system(A) and EPI-β_2AR and ISO-β_2AR systems(B)

RMSDs include the RMSDs of β_2AR relative to itself and ligands to β_2AR.

In the interaction of NE with β_2AR[Fig.4(A)], three hydrogen bonds are formed between each of the catechol hydroxyl groups, amino group and each of residues N293, Y199, N312(the hydrogen bonds are determinate by the FindHBond command of the Chimera program[35]). A salt bridge is founded between D113 and the amino group of NE. Besides polar interaction, residues F289, F290 and Y308 also form strong nonpolar interaction with the aryl of the catechol group, residue Y308 and the catechol group form a strong face-to-face π-stacking interaction at a distance of 0.31 nm.

EPI and ISO display very similar binding modes[Fig.4(B) and (C)]. Residues S203 and S204 respectively form two hydrogen bonds with each of the catechol hydroxyl groups of EPI and one catechol hydroxyl group of ISO, and the difference is that one hydroxyl of ISO and two hydroxyls of EPI form two hydrogen bonds with S203 and S204. NE can form hydrogen bond with residue N312, but EPI and ISO can not. We attribute this to the steric hindrance of methyl group of EPI and *i*-propyl group of ISO. Residue Y308 in NE-β_2AR system shows a strong nonpolar interaction with NE, while in the other systems residue Y308 displays a strong polar interaction with EPI and ISO. Other differences are also found. Residues Y199 and T195 in NE-β_2AR system instead of residues S203 and S204 in EPI-β_2AR and ISO-β_2AR systems directly interact with the agonists, while residues S203 and S204 indirectly interact with NE[Fig.4(A)].

Binding sites of agonists: all the agonists locate in the binding pockets near extracellular region and the first and

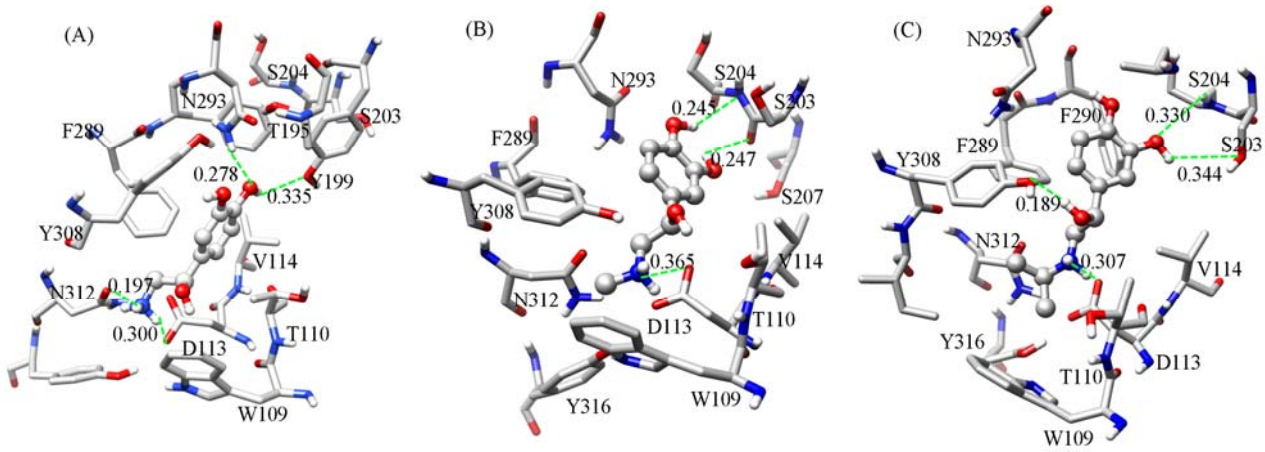

Fig.4 Interaction of agonists with surrounding residues within 0.5 nm

(A) NE; (B) EPI; (C) ISO. The numbers close to dotted green lines represent the lengths(nm) of hydrogen bonds and salt bridges.

second extracellular loops(ECL1 and ECL2, Fig.5). For conveniently comparing the three systems, the interaction residues in the binding sites are listed in Table 1. We can see that the three binding sites share many common residues: T110, D113, V114, F289, F290, N293, Y308, and N312. Experimental studies had proved that D113, F289, F290, and N293 were key residues for constituting the binding pocket[5,36], and theoretical investigations agree with our studies[18,37] well.

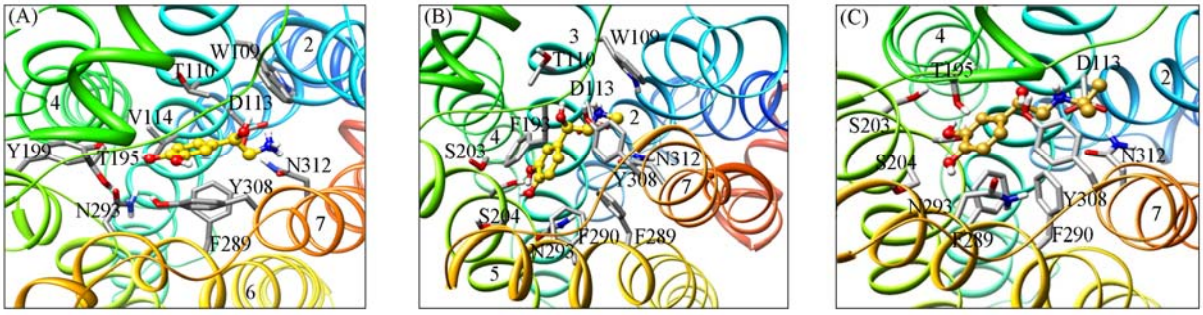

Fig.5 Binding sites of agonists for NE(A), EPI(B) and ISO(C)

The structures of β_2AR are shown in iridescence ribbons. The surrounding residues that strongly interacted with agonists are shown in sticks. Agonists are shown in balls and sticks with the carbon atoms in gold color and other atoms colored by atom type(nitrogen atoms in blue color, oxygen atoms in red color and hydrogen atoms in white color, carbon atoms of protein in gray color). All the conformations of β_2AR are the average structures from the final 2 ns of MD simulation.

Table 1 Interaction residues in the binding cavities of three agonist-β_2AR systems*

Ligand	Directly interactive residues with ligand												
NE	*W109*	T110	D113	*V114*	*F193*	T195			*F289*	*F290*	N293	*Y308*	N312
EPI	*W109*	T110	D113	*V114*	*F193*		S203	S204	*F289*	*F290*	N293	Y308	N312
ISO		T110	D113	*V114*		T195	S203	S204	*F289*	*F290*	N293	Y308	N312

* The residues in italics form nonpolar interaction with β_2AR, while the other residues form polar interaction with β_2AR.

Residues S203 and S204 are in the binding sites of EPI and ISO, and they respectively form strong polar interaction with EPI and ISO. This result agrees with the experimental data[5] well. But in the binding site of NE, the distances between S203, S204 and NE are more than 0.5 nm and weak interactions are formed between them assisted by surrounding water molecules. We refer these differences to the small framework and large mobility of NE. Thus, there is no substituent in the amino group of NE and it can move to the top part of its binding pocket to form strong interaction with T195, Y199, and Y308.

3.2.3 Conformational Changes in Transmembrane Regions

MD simulation may provide useful information about the conformational changes in NE-β_2AR system[Fig.6(A)]. The RMSD value between these two conformations is 0.34 nm. Transmembrane regions(TMs) 2—7 show noticeable movement both in vertical and horizontal directions. In general, TMs 2, 4, and 5 move to the top part and TMs 3, 6 and 7 move to the bottom part of the protein. All the TMs are prone to closing to each other, and the binding cavity is dwindled. TM1 also shows obvious change, but it is situated at the terminal of protein chain, which always move during simulation. Therefore, its motion can not reflect the real situation of protein. Besides, the position of NE shifts to the upper part of the binding site. The loop regions also show great changes, but in MD simulation, the movements of the loop regions are usually mussy.

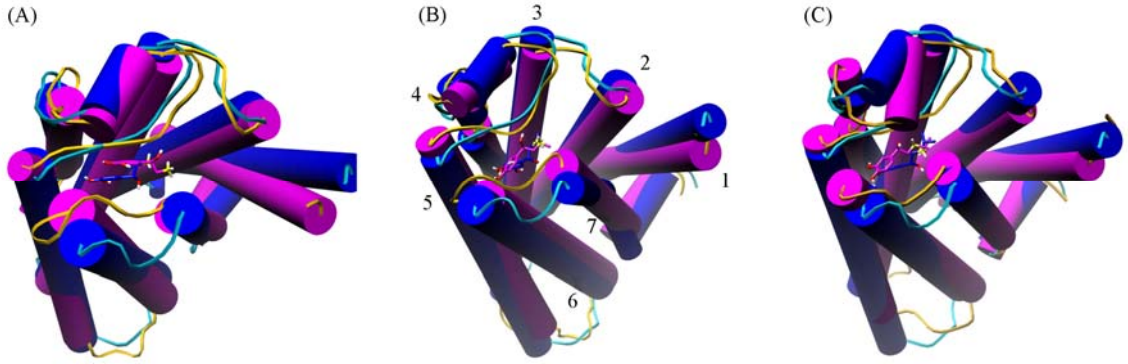

Fig.6 Superposition of structures before and after MD simulation

(A) NE-β_2AR; (B) EPI-β_2AR; (C) ISO-β_2AR. Blue sticks represent the original structures of TMs(before MD simulation), and magenta sticks represent the final structures of TMs after simulation; the loop regions are in cyan and brown lines, respectively.

Conformational changes are also found in the other two systems[Fig.6(B) and(C)]. In EPI-β_2AR, TMs 2 and 5 move to the top part of the protein, and other TMs move to the bottom part. In the ISO-β_2AR system, TMs 2 and 3 show a down movement, and other TMs display upwards movement. The horizontal movement of TMs makes the binding cavities of EPI and ISO decreased. Actually, the motion of TM3 and TM6 was demonstrated by experimental studies[6]. These conformational

changes esepcially the motion of TM6 indicate an important element of the active state of β_2AR[38].

For comparing, we calculated the volumes of binding cavities. Firstly, we should identify the binding cavities; then, we measured the volume of the binding cavities, and all these operations were achieved by 'Measure Volume and Area' command of the Chimera program[35]. The initial volume of the binding cavity of the crystal structure was 0.2684 nm^3. But after binding with NE, EPI and ISO, the volumes decreased to 0.1595, 0.1623 and 0.1956 nm^3, respectively. These decreases of binding cavity derived from the movement of TMs. NE and EPI have very similar structures, while ISO has a larger steric hindrance than NE and EPI, thus the binding cavity for ISO is much bigger than those for others. The movement in TMs derived from the induction of agonists, and different agonists may activate distinct processes from inactive states to active states. Though these three agonists are all catecholamine, and they have little difference in structure, their detailed conformational changes are different. It should be pointed out that this conclusion was not come from a single MD trajectory, but repeated results.

3.2.4 *Water Molecules in Binding Sites*

Water molecules participated in the activation process of β_2AR[11]. We performed MD simulation to investigate it[18—21,39,40]. Some water molecules gradually enter into the binding pocket, and form stable hydrogen bonds with agonist molecules and residues after 20 ns of simulation(Fig.7). In NE-β_2AR system[Fig.7(A)], six water molecules strongly interact with agonist and residues *via* hydrogen bonds with lengths of 0.17—0.22 nm. These water molecules connect residues Y199, F193 and NE, and form hydrogen bond network among the amino group and the alkyl hydroxyl group of NE and residue D113.

In EPI-β_2AR system[Fig.7(B)], four water molecules exist steadily in the binding site and form hydrogen bonds with T110, N312 and EPI, with bond lengths of 0.18—0.23 nm. Because the catechol group of EPI has already formed direct interaction with S203 and S204, no water molecules exist between the catechol group and each of residues S203, S204. But another hydrogen bond is formed between one hydroxyl of the catechol group and a water molecule.

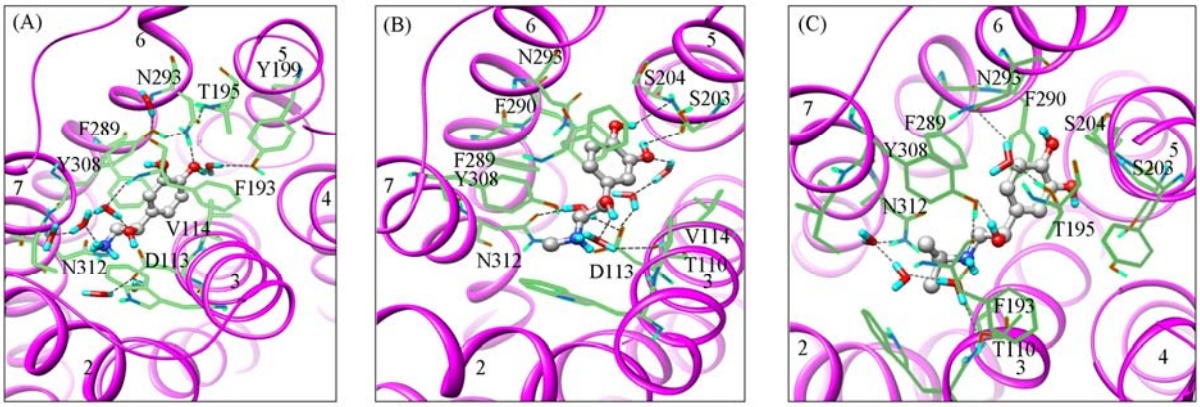

Fig.7 Hydrogen bond networks of water molecules, agonists and surrounding residues

(A) NE-β_2AR system; (B) EPI-β_2AR system; (C) ISO-β_2AR system. For clarity, agonists are in ball and sticks, water molecules in sticks, and surrounding residues in lines. The structure of β_2AR is shown in magenta ribbons; hydrogen atoms, nitrogen atoms, carbon atoms and oxygen atoms are in cyan, blue, gray and red color, respectively. The hydrogen bonds are clearly shown in black dotted lines.

There is no direct interaction between ISO and water molecule in ISO-β_2AR system. All hydrogen bond networks are formed between the surrounding residues and water molecules. Although no direct interaction with ISO exists, water molecules connected T195, N293, T110 and N312 by strong hydrogen bonds with bond lengths of 0.17—0.19 nm. Data show that water molecules enter into the binding sites and mediate the conformational changes of the agonist, neighboring residues, and distant residues.

3.2.5 *Active Elements of Agonist-β_2AR Systems*

To gain the varying degrees from inactive state to active state after MD simulation, intensive studies were performed to the three agonist-β_2AR systems. We examined the changes of the important molecular switches and the conserved DRY motif.

Ionic lock: in GPCRs, there is an ionic lock between TM5 and TM6, and in β_2AR, the ionic lock is between R131 and E268. Experimental studies showed that ionic lock would be broken in the active state of GPCRs[38,41]. As for β_2AR, the ionic lock between R131 and E268 is also broken under the influence of agonists[11]. We found that all the ionic locks of agonist-β_2AR systems are broken which are different from those of the crystal structure[Fig.8(C_1)—(C_3)]. In inverse agonist-β_2AR systems, the ionic locks are very stable[22], therefore, the agonists play important roles in the change of the ionic lock.

Rotamer toggle switch: in the course of conformational change, there is a rotamer toggle switch between W286 and D79, as shown in Fig.8. In crystal structure, residues W286 and D79 are inclined to form hydrogen bond, while in agonist-β_2AR systems, W286 and D79 change their direction and the distance between them is increased. The changes of W286 and D79 trigger the conformational change of TM6 and TM2. And this is why W286 and D79 are called rotamer toggle switch. From Fig.8(B_1)—(B_3), it can be seen that the heterocyclic of W286 has a clockwise rotation by 15°—30°. These latter results are in accordance with the experimental study[42]. In addition, D79 also changes its conformation to help the

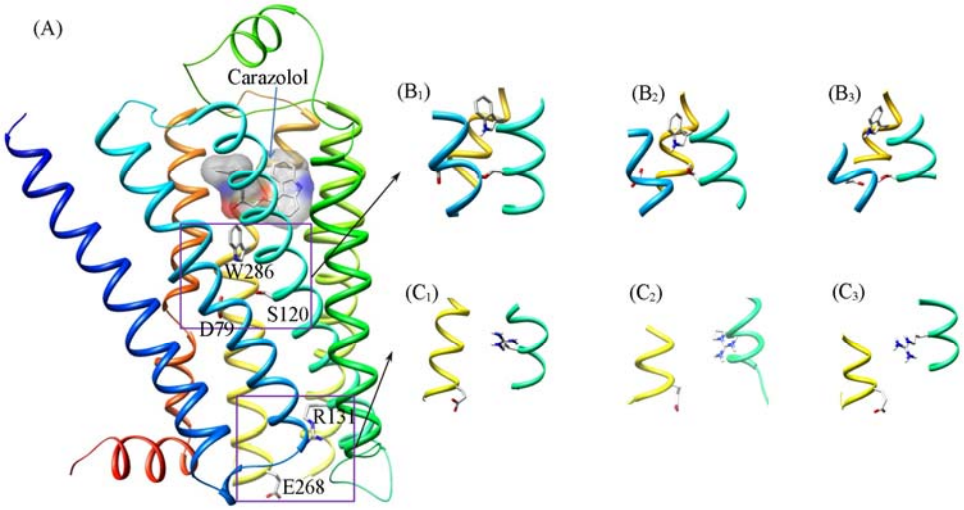

Fig.8 Rotamer toggle switches(D79—W286) and ionic locks(R131—E268) in the crystal structure(A) and agonist-β_2AR systems(B_1—B_3, C_1—C_3)

(B_1) and (C_1) Belong to NE-β_2AR; (B_2) and (C_2) belong to EPI-β_2AR; (B_3) and (C_3) belong to ISO-β_2AR. For clearly displaying the conformation of rotamer toggle switches and ionic lock, only a few ribbon structures of β_2AR are shown.

conformational change of TM6(Fig.6).

DRY motif of β_2AR: in GPCRs, for example, rhodopsin[43] and opsin[38], the conserved E(D)RY regions and ionic lock are very important. In the inactive state[43], the E(D)RY motif forms a more extended hydrogen-bonded network, *i.e.*, 'ionic lock'. While in the active state[38], the ionic lock is broken and the rearranged cytoplasmic ends of TM5 and TM6 are locked by two new interactions. As for β_2AR, the crystal structure is basically in its inactive state[15], and agonists could induce it to the active states. In our agonist-β_2AR systems, we have found that the ionic locks between R131 and E268 are all broken. When examined all the trajectories, we found that the DRY motif has a rearranged interaction(Fig.9). It can be seen that R131 changes its conformation to approach Y326 and Y219, and these changes push the movement of TM6 and TM3. All these conformation changes indicate that β_2AR is near to its active state when bonded with agonist.

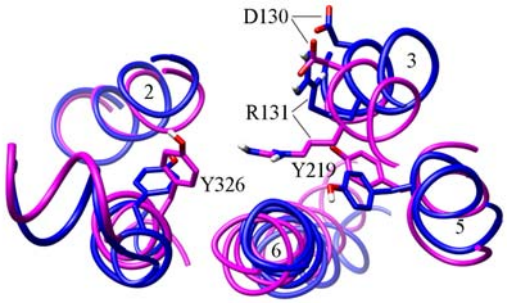

Fig.9 Bottom-view of conformational changes of DRY motif of β_2AR

The ribbons in blue color are the initial structure and the ribbons in magenta color are the likely active structure caught from MD simulation. Residues are colored by element except C atoms which are colored by the ribbon color.

These changes in ionic lock, DRY motif and TMs proved that these agonist-β_2AR systems all come to its active states. Though these agonists have some structural difference, and these agonist-β_2AR systems have different conformational changes in binding sites, TMs or molecular switches, the results are that the binding of agonists near to the extracellula regions of β_2AR induced the activation.

4 Conclusions

In this article, MD simulation, as an important method to study the conformation changes of proteins[44], shows that different agonists induce distinct conformational changes of β_2AR. These conformational changes indicate that β_2AR converted from inactive state to active state. We conclude that agonists contributed to the achievement of the active state by showing the conformation of β_2AR-agonists complexes in the binding sites, TMs, molecular switches, and the conserved DRY motif. We also catch the conformational transition of β_2AR in these three full agonist-β_2AR systems by MD simulation. The possible activation characteristics and active elements are confirmed by three agonist-β_2AR systems.

Acknowledgement

The authors thank Dr. HOU Sen, the Assistant Professor of Polish Academy of Sciences, for insightful discussions and helpful revision to this paper.

References

[1] Kobilka B. K., *Biochim. Biophys. Acta*, **2007**, *1768*(4), 794
[2] Kobilka B. K., Deupi X., *Trends Pharmacol. Sci.*, **2007**, *28*(8), 397
[3] Weitl N., Seifert R., *J. Pharmacol. Exp. Ther.*, **2008**, *327*(3), 760
[4] Ghanouni P., Gryczynski Z., Steenhuis J. J., Lee T. W., Farrens D. L., Lakowicz J. R., Kobilka B. K., *J. Biol. Chem.*, **2001**, *276*(27), 24433
[5] Swaminath G., Xiang Y., Lee T. W., Steenhuis J., Parnot C., Kobilka B. K., *J. Biol. Chem.*, **2004**, *279*(1), 686
[6] Gether U., Lin S., Ghanouni P., Ballestreos J. A., Weinstein H., Kobilka B. K., *EMBO J.*, **1997**, *16*(22), 6737
[7] Yao X. J., Parnot C., Deupi X., Ratnala V. R. P., Swaminath G., Farrens D., Kobilka B., *Nat. Chem. Biol.*, **2006**, *2*(8), 417
[8] Granier S., Kim S., Shafer A. M., Ratnala V. R. P., Fung J. J., Zare

R. N., Kobilka B., *J. Biol. Chem*., **2007**, *282*(18), 13895

[9] Ghanouni P., Steenhuis J. J., Farrens D. L., Kobilka B. K., *Proc. Natl. Acad. Sci. USA*, **2001**, *98*(11), 5997

[10] Swaminath G., Deupi X., Lee T. W., Zhu W., Thian F. S., Kobilka T. S., Kobilka B., *J. Biol. Chem*., **2005**, *280*(23), 22165

[11] Bhattacharya S., Hall S. E., Li H., Vaidehi N., *Biophys. J*., **2008**, *94*(6), 2027

[12] Kobilka B., Schertler G. F. X., *Trends Pharmacol. Sci*., **2008**, *29*(2), 79

[13] Chandramoorthi G. D., Piramanayagam S., Marimuthu P., *J. Mol. Model*., **2008**, *14*(9), 849

[14] Rasmussen S. G. F., Choi H. J., Rosenbaum D. M., Kobilka T. S., Thian F. S., Edwards P. C., Burghammer M., Ratnala V. R. P., Sanishvili R., Fischetti R. F., Schertler G. F. X., Weis W. I., Kobilka B. K., *Nature*, **2007**, *450*(7168), 383

[15] Cherezov V., Rosenbaum D. M., Hanson M. A., Rasmussen S. G. F., Thian F. S., Kobilka T. S., Choi H. J., Kuhn P., Weis W. I., Kobilka B. K., Stevens R. C., *Science*, **2007**, *318*(5854), 1258

[16] Palczewski K., Kumasaka T., Hori T., Behnke C. A., Motoshima H., Fox B. A., Le Trong I., Teller D. C., Okada T., Stenkamp R. E., Yamamoto M., Miyano M., *Science*, **2000**, *289*(5480), 739

[17] Soriano-Ursua M. A., Trujillo-Ferrara J. G., Correa-Basurto J., *J. Mol. Model*., **2009**, *15*(10), 1203

[18] Huber T., Menon S., Sakmar T. P., *Biochemistry*, **2008**, *47*(42), 11013

[19] Dror R. O., Arlow D. H., Borhani D. W., Jensen M. O., Piana S., Shaw D. E., *Proc. Natl. Acad. Sci. USA*, **2009**, *106*(12), 4689

[20] Vanni S., Neri M., Tavernelli I., Rothlisberger U., *Biochemistry*, **2009**, *48*(22), 4789

[21] Han D. S., Wang S. X., Weinstein H., *Biochemistry*, **2008**, *47*(28), 7317

[22] Rasmussen S. G. F., Choi H. J., Fung J. J., Pardon E., Casarosa P., Chae P. S., DeVree B. T., Rosenbaum D. M., Thian F. S., Kobilka T. S., *Nature*, **2011**, 469(7329), 175

[23] Periole X., Huber T., Marrink S. J., Sakmar T. P., *J. Am. Chem. Soc*., **2007**, *129*(33), 10126

[24] Wess J., Han S. J., Kim S. K., Jacobson K. A., Li J. H., *Trends Pharmacol. Sci*., **2008**, *29*(12), 616

[25] Frisch M. J., Trucks G. W., Schlegel H. B., Scuseria G. E., Robb M. A., Cheeseman J. R., Montgomery J. A. Jr., Vreven T., Kudin K. N., Burant J. C., Millam J. M., Iyengar S. S., Tomasi J., Barone V., Mennucci B., Cossi M., Scalmani G., Rega N., Petersson G. A., Nakatsuji H., Hada M., Ehara M., Toyota K., Fukuda R., Hasegawa J., Ishida M., Nakajima T., Honda Y., Kitao O., Nakai H., Klene M., Li X., Knox J. E., Hratchian H. P., Cross J. B., Bakken V., Adamo C., Jaramillo J., Gomperts R., Stratmann R. E., Yazyev O., Austin A. J., Cammi R., Pomelli C., Ochterski J. W., Ayala P. Y., Morokuma K., Voth G. A., Salvador P., Dannenberg J. J., Zakrzewski V. G., Dapprich S., Daniels A. D., Strain M. C., Farkas O., Malick D. K., Rabuck A. D., Raghavachari K., Foresman J. B., Ortiz J. V., Cui Q., Baboul A. G., Clifford S., Cioslowski J., Stefanov B. B., Liu G., Liashenko A., Piskorz P., Komaromi I., Martin R. L., Fox D. J., Keith T., Al-Laham M. A., Peng C. Y., Nanayakkara A., Challacombe M., Gill P. M. W., Johnson B., Chen W., Wong M. W., Gonzalez C., Pople J. A., *Gaussian 03*, *Revision C.02*, Gaussian Inc., Wallingford CT, **2004**

[26] Standfuss J., Xie G. F., Edwards P. C., Burghammer M., Oprian D. D., Schertler G. F. X., *J. Mol. Biol*., **2007**, *372*(5), 1179

[27] Warne T., Serrano-Vega M. J., Baker J. G., Moukhametzianov R., Edwards P. C., Henderson R., Leslie A. G. W., Tate C. G., Schertler G. F. X., *Nature*, **2008**, *454*(7203), 486

[28] Jaakola V. P., Griffith M. T., Hanson M. A., Cherezov V., Chien E. Y. T., Lane J. R., Ijzerman A. P., Stevens R. C., *Science*, **2008**, *322*(5905), 1211

[29] Rubenstein L. A., Zauhar R. J., Lanzara R. G., *J. Mol. Graph. Model*., **2006**, *25*(4), 396

[30] Ballesteros J. A., Jensen A. D., Liapakis G., Rasmussen S. G. F., Shi L., Gether U., Javitch J. A., *J. Biol. Chem*., **2001**, *276*(31), 29171

[31] Morris G. M., Goodsell D. S., Halliday R. S., Huey R., Hart W. E., Belew R. K., Olson A. J., *J. Comput. Chem*., **1998**, *19*(14), 1639

[32] Sanner M. F., *J. Mol. Graph. Model*., **1999**, *17*(1), 57

[33] Lindahl E., Hess B., van der Spoel D., *J. Mol. Model*., **2001**, *7*(8), 306

[34] Schuttelkopf A. W., van Aalten D. M. F., *Acta Crystallogr. D*, *Biol. Crystallogr*., **2004**, *60*, 1355

[35] Pettersen E. F., Goddard T. D., Huang C. C., Couch G. S., Greenblatt D. M., Meng E. C., Ferrin T. E., *J. Comput. Chem*., **2004**, *25*(13), 1605

[36] Wieland K., Zuurmond H. M., Krasel C., IJzerman A. P., Lohse M. J., *Proc. Natl. Acad. Sci. USA*, **1996**, *93*, 9276

[37] Xhaard H., Rantanen V. V., Nyronen T., Johnson M. S., *J. Med. Chem*., **2006**, *49*(5), 1706

[38] Park J. H., Scheerer P., Hofmann K. P., Choe H. W., Ernst O. P., *Nature*, **2008**, *454*(7201), 183

[39] Spijker P., Vaidehi N., Freddolino P. L., Hilbers P. A. J., Goddard W. A., *Proc. Natl. Acad. Sci. USA*, **2006**, *103*(13), 4882

[40] Vaidehi N., Floriano W. B., Trabanino R., Hall S. E., Freddolino P., Choi E. J., Zamanakos G., Goddard W. A., *Proc. Natl. Acad. Sci. USA*, **2002**, *99*(20), 12622

[41] Bhattacharya S., Hall S. E., Vaidehi N., *J. Mol. Biol*., **2008**, *382*(2), 539

[42] Shi L., Liapakis G., Xu R., Guarnieri F., Ballesteros J. A., Javitch J. A., *J. Biol. Chem*., **2002**, *277*, 40989

[43] Okada T., Sugihara M., Bondar A. N., Elstner M., Entel P., Buss V., *J. Mol. Biol*., **2004**, *342*, 571

[44] Liu X., Li X., Teng H., Xiu Z., *Chem. Res. Chinese Universities*, **2009**, *25*(4), 560